

Truncation Artifact Reduction in Cone-beam CT using Mixed One-bit Compressive Sensing

Xiaolin Huang^{*†}, Yan Xia[‡], Yixing Huang[†], Joachim Hornegger[†], Jie Yang^{*}, Andreas Maier[†]

^{*}Institute of Image Processing and Pattern Recognition, Shanghai Jiao Tong University, Shanghai, China

[†]Pattern Recognition Lab, Friedrich-Alexander-Universität Erlangen-Nürnberg, Erlangen, Germany

[‡]Department of Radiology, Stanford University, Stanford, USA

Email: xiaolinhuang@sjtu.edu.cn

Abstract—In cone-beam computed tomography (CT), it is not uncommon that the acquired projection data are truncated due to either limited detector size or intentionally reduced field of view (FOV) for dose reduction. The resulting truncation is not compatible to conventional reconstruction algorithms and thus leads to truncation artifacts, e.g., the cupping effect towards the boundary of the FOV and incorrect offset in the Hounsfield unit values of reconstructed voxels. Typical truncation artifact correction schemes involve estimating the truncated projection by extrapolation, e.g., water cylinder extrapolation. But the estimation is heuristic and may not always be accurate. In this paper, we propose to estimate the upper bound of missing data and then use the mixed one-bit compressive sensing (M1bit-CS) to compensate truncation artifacts. Bound estimation is much easier and more accurate than projection value estimation and M1bit-CS yields good reconstruction capability from one-bit information, i.e., the bounding inequality. In numerical experiments on both a phantom and a reprojection of a clinical image, the proposed method shows superior reconstruction results over the standard water cylinder extrapolation.

Index Terms—Truncation Correction, Compressive Sensing, One-bit Compressive Sensing, C-arm, X-ray.

I. INTRODUCTION

In cone-beam computed tomography (CT) systems, 3D volumetric images are typically obtained using analytical filtered-backprojection (FBP) reconstruction algorithms, such as the Feldkamp-Davis-Kress (FDK, [1]) method, which is efficient and robust, yielding superior reconstructions in practice. However, it cannot handle the laterally truncated projection data due to its non-local filter processing. The data truncation occurs very often when the imaged object is larger than the detector size or X-ray beams are intentionally collimated into a small diagnostic of interest to reduce patient dose. Consequently, in these scenarios, the direct application of FDK on truncated data leads to severe truncation artifacts, manifesting as a bright ring/cupping at the edge of truncation, and incorrect Hounsfield unit (HU) values. These artifacts considerably contaminate the final reconstruction results.

One way to reduce truncation artifacts is based on ramp filter decomposition; see, e.g. [2] [3] [4]. Another popular category of truncation artifact correction methods is based on estimating the missing data using heuristic extrapolation, such as symmetric mirroring of projection images [5], water

cylinder extrapolation [6], square root extrapolation [7] and hybrid extrapolation [8]. Although these methods can be carried out without prior information, they rely on heuristics. Their accuracy highly depends on the level of truncation. In contrast, [9] and [10] suggested that patient size and shape information can be obtained from a prior low-dose CT scan if available. By forward-projection of this prior CT volume, the collimated region in the region of interest acquisition can be extended in an accurate manner. These methods, however, require a certain clinical workflow, on which one cannot always rely.

Inspired by the recent progress on one-bit compressive sensing (1bit-CS, see, e.g., [11], [12]), in this paper we propose to estimate the upper bound of missing data in the CT sinogram and then use the mixed one-bit compressive sensing (M1bit-CS), which is newly developed by [13], to compensate truncation artifacts. Bound estimation is much easier and more accurate than projection value estimation (that other extrapolation aim to restore) and M1bit-CS yields good reconstruction capability from one-bit information, i.e., the bounding inequality. Compared with extrapolation based methods, M1bit-CS requires only bound estimation. Compared with total variation (TV) based CS methods, such as [14] and [15], we mine knowledge additionally from projection bounds that is very helpful to reduce truncation artifacts.

The rest of this paper is organized as follows. In Section II, M1bit-CS together with a bound estimation method for truncation correction are established. Section III evaluates the proposed methods on simulated clinical data. A conclusion is given to end this paper in Section IV.

II. M1BIT-CS FOR TRUNCATION CORRECTION

A. Data Truncation in Cone-beam CT

The X-ray transform of an object f is denoted by R . Then the ideal acquired projection is

$$y = Rf. \quad (1)$$

However, due to the limited detector size, a part of the projections cannot be observed. As an intuitive example, let us consider a phantom displayed by Fig.1(a), where the field-of-view (FOV) is marked by the dashed yellow circle. To reconstruct issues in the FOV, only the incomplete sinogram between the two green dashed lines (see Fig.1(c)) is needed.

This work is partially supported by Alexander von Humboldt Foundation and National Natural Science Foundation of China (61603248).

We introduce a boolean indicator vector Φ to represent the truncation situation: $\Phi_i = 0$ stands for an observed projection and $\Phi_i = 1$ means a truncated projection. Simply applying the standard FBP leads to the image in Fig.1(b), where one can find significant artifacts near the FOV boundary and the structure outside the FOV is totally lost.

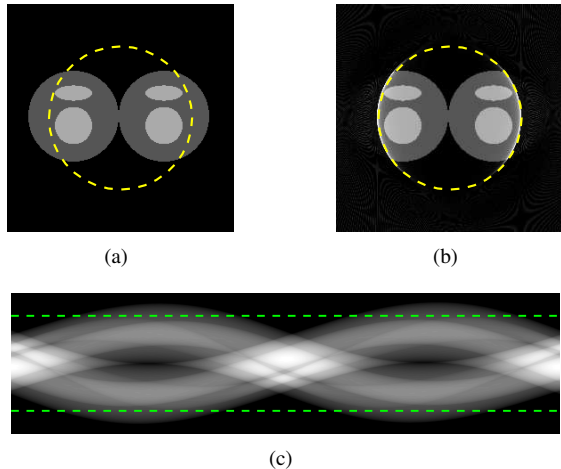


Fig. 1. (a) Phantom and the FOV marked by the yellow dashed circle; (b) reconstructed result by FBP; (c) the projections and its truncation marked by the green dashed lines. The display window is $[-1000, 2000]$ HU.

B. Mixed One-bit Compressive Sensing

To correct truncation artifacts, the typical idea is to estimate the truncated projections by extrapolation. For example, one can assume the missing data as line integrals of a partial water cylinder as [6]. The main difficulty is that those extrapolation methods are only accurate when the object structure is simple. In this paper, we propose to estimate the upper bound of the missing projections. Compared with value estimation for $(\mathbf{Rf})_i$, bound estimation that finds s_i such that $s_i \geq (\mathbf{Rf})_i$ is more convenient. If the bound s_i is found, a recent method, called mixed one-bit compressive sensing (M1bit-CS, [13]), is applicable to reconstruct images.

M1bit-CS is based on compressive sensing (CS) and one-bit compressive sensing (1bit-CS). The interested reader is referred to [16] [17] [18] for CS and [11] [12] [19] [20] for 1bit-CS. Its reconstruction process acquires information from two parts. For the regular projections, i.e., $\Phi_i = 0$, we can use the observed value y_i . For the truncated projections, i.e., $\Phi_i = 1$, we use its upper bound s_i . Another important prior-knowledge is that the image is sparse in its gradient domain, which follows the use of total variation (TV) regularization. Summarizing the discussions, we come to the following M1bit-CS model,

$$\min_{\mathbf{f}} \quad \mu \|\mathbf{f}\|_{\text{TV}} + \frac{1}{2} \sum_{i:\Phi_i=0} ((\mathbf{Rf})_i - y_i)^2 + \lambda \sum_{i:\Phi_i=1} \max\{0, (\mathbf{Rf})_i - s_i\}. \quad (2)$$

This is a convex model and an alternating direction method of multipliers (ADMM, see, e.g., [21]) was designed by [13] to solve (2). Basically, we need to introduce a bound error vector

\mathbf{e} and Lagrangian multipliers α . Then (2) can be solved via the following iterative algorithm

Algorithm 1: An ADMM for M1bit-CS ([13])

Initialize: $\mathbf{f} := \mathbf{0}$, $\mathbf{e} := \mathbf{0}$, $\alpha := \mathbf{0}$, $k := 0$, and $\theta > 0$;
repeat

- Update \mathbf{e} as

$$\mathbf{e} := \mathbb{S}(\mathbf{s} - \mathbf{Rf} - \alpha/\theta, \lambda/\theta),$$

where \mathbb{S} is the shrinkage operator induced from a componentwise operator, i.e.,

$$(\mathbb{S}(\mathbf{g}, \rho))_i := \begin{cases} g_i - \rho, & \text{if } g_i \geq \rho, \\ 0, & \text{if } |g_i| < \rho, \\ g_i + \rho, & \text{if } g_i \leq -\rho; \end{cases}$$

- Update \mathbf{f} by solving

$$\min_{\mathbf{f}} \quad \mu \|\mathbf{f}\|_{\text{TV}} + \frac{1}{2} \sum_{i:\Phi_i=0} ((\mathbf{Rf})_i - y_i)^2 + \alpha^\top \mathbf{Rf} + \frac{\theta}{2} \|\mathbf{e} - \mathbf{s} + \mathbf{Rf}\|_2^2,$$

which is a typical minimization problem involving a TV plus a quadratic term and there are many existing algorithms to use;

- Update α as in Gauss-Siedel style, i.e.,

$$\alpha := \alpha + \theta(\mathbf{e} - \mathbf{s} - \mathbf{Rf});$$

- $k := k + 1$;

until convergence or k reaches the max iterations;

Output: reconstructed image \mathbf{f} .

C. Iterative Bound Estimation

In this section we show how to estimate upper bound s_i used in (2), which is a key point of the proposed method. We introduce an iterative bound estimation (IBE) scheme. It starts from the image reconstructed by FBP, denoted by $\tilde{\mathbf{f}}$. Due to the truncation, $\tilde{\mathbf{f}}$ is only reliable in a small region, called a reliable region (RER). In fact, even in this region, $\tilde{\mathbf{f}}$ is not accurate due to the existence of offset occurred by truncation. Fortunately, this offset always makes the values greater and hence it can be used for estimating the upper bound. We artificially construct a maximum image $\bar{\mathbf{f}}$ that preserves the elements of $\tilde{\mathbf{f}}$ in RER and takes the maximum value outside RER. Then $s_i = (\mathbf{R}\bar{\mathbf{f}})_i$ can be calculated for each $i : \Phi_i = 1$. With s_i , which obviously is an upper bound of the i -th projection, we can use M1bit-CS (2) to reconstruct an image and repeat the above process to update the upper bound. Notice that at the beginning, RER should be smaller than the FOV to guarantee its accuracy. With the iteration increasing, larger parts are well estimated and then RER grows. As an example, let us consider reconstruction from projections Fig.1(c). The initial $\bar{\mathbf{f}}$ is displayed in Fig.2(a), where the data inside RER preserve values from the reconstructed result of FBP. From the initial image, applying this IBE scheme and M1bit-CS (M1bit-CS-IBE for short), we can successfully recover the phantom from truncated projections. Take the data in Fig.1(c) as an example,

the reconstructed image is given by Fig.2(b), of which the recovery quality is significantly improved from that of FBP not only in the FOV but also outside the FOV. The improvement can also be quantitatively observed from the root-mean-square error (RMSE) as reported in Fig.2.

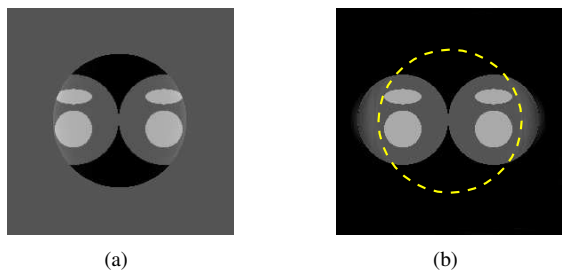


Fig. 2. (a) Initial \hat{f} for bound estimation; it takes \hat{f} in RER and maximal possible value outside RER; (b) reconstruction result obtained by M1bit-CS-IBE. The display window is $[-1000, 2000]$ HU. In the FOV, the reconstruction is quite accurate with RMSE (in HU) being 4.175. Outside the FOV, the RMSE is 40.77. The performance is largely improved from FBP, which outputs an image with RMSE being 262.4 and 275.1 inside and outside the FOV, respectively.

III. EXPERIMENTS AND RESULTS

In the previous sections, we established M1bit-CS-IBE and applied it on a phantom. This section further evaluates M1bit-CS-IBE on a clinical head dataset, which is acquired with a Siemens Artis zee angiographic C-arm system (Siemens Healthcare GmbH, Forchheim, Germany). In this experiment, we choose one slice of a 3D clinical head dataset as the ground truth image Fig.4(a), where the FOV is marked by the dashed yellow circle, and reproject it to simulate the acquired sinogram data (Fig.3) in a fan-beam system with the following trajectory parameters: image size is 256×256 , pixel length is 1 mm. The intensity values for the background, soft tissue, and bones are -1000 HU, 0 HU, and 2000 HU, respectively. Regarding the fan-beam trajectory parameters, the source-to-isocenter distance is 750 mm and isocenter-to-detector distance is 450 mm. The angular step is 1 degree and the total scan range is 360 degrees.

The equal-spaced detector length s_{\max} is 620 mm with the pixel length 1 mm. We simulate a truncation of 160 mm, i.e., only the 460 mm in the center can be observed. The truncated projections are shown in Fig. 3(b). We first apply FBP to reconstruct the image and show its result in Fig.4(b), which has a bright circle in the boundary of the FOV and has almost no structure information outside the FOV. Applying the FBP-WCE [6] that utilizes water cylinder extrapolation to remedy missing projections caused by truncation can improve the performance. Especially in the FOV, the reconstruction is quite accurate, as plotted by Fig.4(c). At last, we use the proposed M1bit-CS-IBE on this truncated data and the result is given in Fig.4(d). Within the FOV, the reconstruction accuracy is quite high, which is also verified by the RMSEs. Moreover, M1bit-CS-IBE can even recover tissues beyond the FOV, e.g., the nose and the ears are well reconstructed, indicating M1bit-CS-IBE a very promising truncation correction method.

When the truncation becomes worse, e.g., in Fig.3(c), there is only a 260 mm detectable range, the truncation artifacts,

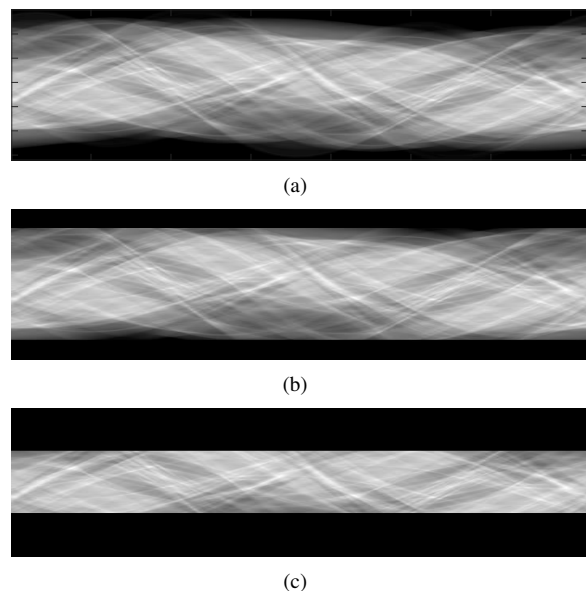


Fig. 3. Sinogram of clinical data displayed in Fig.4(a): (a) Full projection; (b) Truncated projection with the detectable range 460 mm; (c) Truncated projection with the detectable range 260 mm.

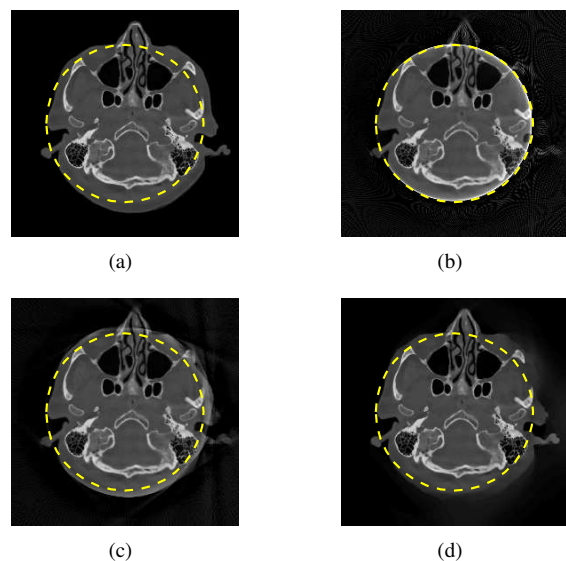


Fig. 4. Image reconstructed from the truncated sinogram shown in Fig.3(b) with different algorithms; the FOV is marked by dashed yellow circle: (a) ground truth; (b) FBP; (c) FBP-WCE; (d) M1bit-CS-IBE. The display window is $[-1000, 2000]$ HU. The RMSEs (in HU) inside the FOV are 317.4 (FBP), 50.25 (FBP-WCE), and 33.71 (M1bit-CS-IBE). Outside the FOV, the RMSEs are 328.0 (FBP), 256.1 (FBP-WCE), and 116.3 (M1bit-CS-IBE).

including cupping effect and incorrect offset, are more significant. Fig.5(b) displays the reconstructed result of FBP-WCE, which failed to get good reconstruction outside the FOV. Even for this severe truncation, the proposed method can nicely reduce the truncation artifacts within the FOV, as displayed in Fig.5(d), where issues beyond the FOV are partially reconstructed as well. To highlight the role of one-bit measurements, we set $\lambda = 0$ in (2), for which SART together with TV minimization can be used. For the reduced model, the proposed iterative bound estimation scheme is still applicable, thus, the whole process is denoted as SART-

TV-IBE. Comparing M1bit-CS-IBE and SART-TV-IBE, one can observe the improvement of using one-bit measurements: RMSE inside the FOV is reduced from 200.9 to 100.9.

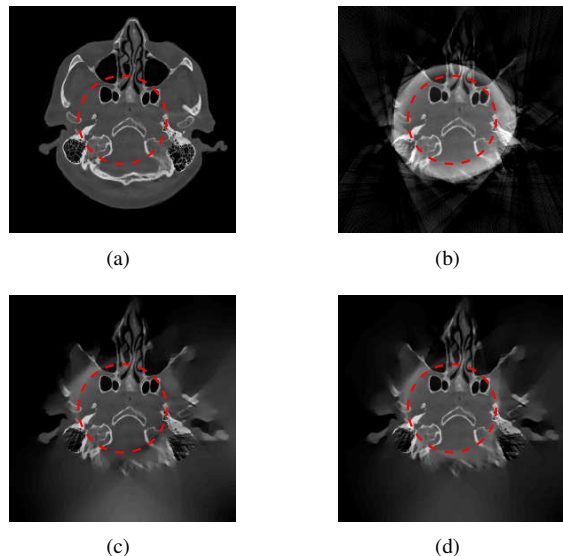


Fig. 5. Image reconstructed from the truncated sinogram shown in Fig.3(c) with different algorithms; the FOV is marked by dashed red circle: (a) ground truth; (b) FBP-WCE; (c) SART-TV-IBE; (d) M1bit-CS-IBE. The display window is $[-1000, 2000]$ HU. The RMSEs (in HU) inside the FOV are 258.8 (FBP-WCE), 200.9 (SART-TV-IBE), and 100.9 (M1bit-CS-IBE). Outside the FOV, the RMSEs are 521.4 (FBP-WCE), 256.1 (SART-TV-IBE), and 223.6 (M1bit-CS-IBE).

IV. CONCLUSION

In this paper, we considered truncation correction for cone-beam CT reconstruction. Based on the iterative bound estimation, we use the mixed one-bit compressive sensing, which can efficiently mine knowledge from both regular and truncated projections. This method is evaluated on a phantom and a simulated clinical image. Compared to the existing truncation correction methods, M1bit-CS-IBE illustrates very promising performance: in the FOV, regular truncation artifacts are nicely removed; outside the FOV, some issues can be reconstructed as well. Further study will be focused on estimating the upper bound more accurate, e.g., we can use extrapolation for bound estimation or design a mask which covers the whole object.

REFERENCES

- [1] L. Feldkamp, L. Davis, and J. Kress, "Practical cone-beam algorithm," *Journal of the Optical Society of America A*, vol. 1, no. 6, pp. 612–619, 1984.
- [2] A. Maier, B. Scholz, and F. Dennerlein, "Optimization-based Extrapolation for Truncation Correction," in *Proceedings of the Second International Conference on Image Formation in X-ray Computed Tomography*, F. Noo, Ed., Salt Lake City, Utah, USA, 2012, pp. 390–394. [Online]. Available: <http://www5.informatik.uni-erlangen.de/Forschung/Publikationen/2012/Maier12-OEF.pdf>
- [3] F. Dennerlein and A. Maier, "Approximate truncation robust computed tomography-ATRACT," *Physics in Medicine and Biology*, vol. 58, no. 17, pp. 6133–6148, 2013.
- [4] Y. Xia, H. Hofmann, F. Dennerlein, K. Müller, C. Schwemmer, S. Bauer, G. Chintalapani, P. Chinnadurai, J. Hornegger, and A. Maier, "Towards clinical application of a laplace operator-based region of interest reconstruction algorithm in C-arm CT," *IEEE Transactions on Medical Imaging*, vol. 33, no. 3, pp. 593–606, 2014.

- [5] B. Ohnesorge, T. Flohr, K. Schwarz, J. Heiken, and K. Bae, "Efficient correction for CT image artifacts caused by objects extending outside the scan field of view," *Medical Physics*, vol. 27, no. 1, pp. 39–46, 2000.
- [6] J. Hsieh, E. Chao, J. Thibault, B. Grekowitz, A. Horst, S. McOlash, and T. J. Myers, "A novel reconstruction algorithm to extend the CT scan field-of-view," *Medical Physics*, vol. 31, no. 9, pp. 2385–2391, 2004.
- [7] K. Sourbelle, M. Kachelrieß, and W. A. Kalender, "Reconstruction from truncated projections in CT using adaptive detruncation," *European Radiology*, vol. 15, no. 5, pp. 1008–1014, 2005.
- [8] M. Zellerhoff, B. Scholz, E.-P. Ruehrnschopf, and T. Brunner, "Low contrast 3D reconstruction from C-arm data," in *Medical Imaging. International Society for Optics and Photonics*, 2005, pp. 646–655.
- [9] J. Wiegert, M. Bertram, T. Netsch, J. Wulff, J. Weese, and G. Rose, "Projection extension for region of interest imaging in cone-beam CT," *Academic Radiology*, vol. 12, no. 8, pp. 1010–1023, 2005.
- [10] D. Kolditz, Y. Kyriakou, and W. A. Kalender, "Volume-of-interest (VOI) imaging in C-arm flat-detector CT for high image quality at reduced dose," *Medical Physics*, vol. 37, no. 6, pp. 2719–2730, 2010.
- [11] P. T. Boufounos and R. G. Baraniuk, "1-bit compressive sensing," in the *42nd Annual Conference on Information Sciences and Systems*. IEEE, 2008, pp. 16–21.
- [12] M. Yan, Y. Yang, and S. Osher, "Robust 1-bit compressive sensing using adaptive outlier pursuit," *IEEE Transactions on Signal Processing*, vol. 60, no. 7, pp. 3868–3875, 2012.
- [13] X. Huang, Y. Xia, L. Shi, Y. Huang, M. Yan, J. Hornegger, and A. Maier, "Mixed one-bit compressive sensing with applications to overexposure correction for CT reconstruction," *arXiv:1701.00694*, 2017.
- [14] H. Yu and G. Wang, "Compressed sensing based interior tomography," *Physics in Medicine and Biology*, vol. 54, no. 9, p. 2791, 2009.
- [15] E. Katsevich, A. Katsevich, and G. Wang, "Stability of the interior problem with polynomial attenuation in the region of interest," *Inverse Problems*, vol. 28, no. 6, p. 065022, 2012.
- [16] E. J. Candès and T. Tao, "Decoding by linear programming," *IEEE Transactions on Information Theory*, vol. 51, no. 12, pp. 4203–4215, 2005.
- [17] D. L. Donoho, "Compressed sensing," *IEEE Transactions on Information Theory*, vol. 52, no. 4, pp. 1289–1306, 2006.
- [18] Y. C. Eldar and G. Kutyniok, *Compressed Sensing: Theory and Applications*. Cambridge University Press, 2012.
- [19] Y. Plan and R. Vershynin, "Robust 1-bit compressed sensing and sparse logistic regression: A convex programming approach," *IEEE Transactions on Information Theory*, vol. 59, no. 1, pp. 482–494, 2013.
- [20] L. Zhang, J. Yi, and R. Jin, "Efficient algorithms for robust one-bit compressive sensing," in *Proceedings of the 31st International Conference on Machine Learning*, 2014, pp. 820–828.
- [21] S. Boyd, N. Parikh, E. Chu, B. Peleato, and J. Eckstein, "Distributed optimization and statistical learning via the alternating direction method of multipliers," *Foundations and Trends in Machine Learning*, vol. 3, no. 1, pp. 1–122, 2011.